

PHYSICAL CHEMISTRY
OF WATER TREATMENT PROCESSES

Electrochemical Detection of Hg(II) in Environmental Water Samples Based on Multiwalled Carbon Nanotube-Reduced Graphene Oxide Hybrid Film¹

L. Lu^{a,*} and Y. H. Zheng^b

^aCollege of Materials and Environmental Engineering, Hangzhou Dianzi University, China

^bInstitute of Botany, Jiangsu Province and Chinese Academy of Sciences, Nanjing Botanical Garden, China

*e-mail: fuli@hdu.edu.cn

Received November 27, 2014

Abstract—In this work, we describe the fabrication of an electrochemical sensor for the detection of Hg²⁺ in various water samples. The electrochemical sensor is fabricated on an indium tin oxide (ITO) modified with multi-walled carbon nanotubes (MWCNT) and reduced graphene oxide (RGO) hybrid film. The MWCNT was firstly dispersed using graphene oxide (GO) as dispersant. After coating on the ITO, the GO was then electrochemically reduced to RGO. The obtained thin film was characterized by scanning electron microscope (SEM), FTIR, Raman spectroscopy and 3D optical surface profiler. Cyclic voltammetry and differential pulse voltammetry were employed to investigate the electrocatalytic performance towards the Hg²⁺ oxidation. Under optimum conditions, the proposed sensor showed a wider linear range at Hg(II) concentrations of 0.05–150 nM. The limit of detection was calculated to be 0.05 nM.

DOI: 10.3103/S1063455X18040069

Keywords: electrochemical sensor, Hg(II) detection, graphene oxide, carbon nanotube, water pollution.

INTRODUCTION

As is well known, Hg²⁺ ions can cause a number of health problems such as brain damage and kidney failure even at very low concentration [1–3]. Also, it accounts for the majority of toxicity events in microorganisms and other species in the environment. Because the Hg²⁺ ions are a major and dangerous contaminant in environmental and potable water, development of an effective analytical method is strongly demanded. So far, many analytical methods have been developed for the detection of Hg²⁺, such as surface enhanced Raman spectroscopy [4], fluorescent method [5], colorimetric sensor [6], photoelectrochemical biosensor [7] and electrochemical sensor [8–16]. Among these approaches, due to the relatively high efficiency, sensitivity, lower cost and simplicity, electrochemical method have become an important investigation domain for Hg²⁺ detection. In order to enhance the electrochemical performance of the electrode, many materials have been used as electrode modifier. For example, the authors [17] demonstrated using a three-dimensional-gap-net in an Au–thiol coordination polymer for electrochemical detection of Hg²⁺. It is known a palladium oxide/graphite composite electrode for determining Hg²⁺ [18].

Carbon nanotubes are often used for construction of electrochemical sensors due to their high strength and flexibility, high thermal and electrical conductivity [19–21]. As an important species, multi-walled carbon nanotubes (MWCNT) have been used for incorporation with other materials to form composites to enhance the electrocatalytic properties of the electrode. For example, Zhang and co-workers reported a polypyrrole-imprinted electrochemical sensor based on SnO₂-MWCNT film modified carbon electrode for the determination of oleanolic acid. On the other hand, graphene, a two-dimensional sp²-hybridized carbon material, has attracted attention of various research groups because its excellent charge transport mobility, large specific surface area, high electrocatalytic activity and low cost [22–30]. Due to these properties, graphene has been used as a new carbon based electrocatalysts for sensing applications. Therefore, attempts to combine graphene with MWCNT is expected to generate a suitable electrode material for Hg²⁺ sensing application. In this work, we fabricated an electrochemical Hg²⁺ sensor based on MWCNT-reduced graphene oxide (RGO) modified

¹ The text was submitted by the authors in English.

indium tin oxide (ITO). The proposed sensor exhibited an excellent performance towards detection of Hg^{2+} ions in various water samples.

EXPERIMENTAL

Synthetic graphite (average particle diameter $< 20 \mu\text{m}$) was purchased from Sigma-Aldrich. MWCNT (purity 95%, diameters 40–60 nm, length 1–2 μm) was purchased from Shenzhen Nanotech Port Co. Ltd. (China). All other chemicals used were analytical grade reagents without further purification. Milli-Q water (18.2 $\text{M}\Omega \text{cm}$) was used throughout the experiments.

Graphene oxide (GO) was firstly prepared with the modified Hummers method with little modifications [31–34]. The MWCNT-GO dispersion was prepared by adding GO (80 mg) into 160 ml water through 1 h ultrasound under ambient condition, then 20 mg MWCNT was introduced to the dispersion for further 3 h ultrasound until a homogeneous black suspension was achieved. After that, 1 mL MWCNT-GO dispersion was dropped onto the ITO substrate and dried at room temperature.

The electro-reduction of MWCNT-GO to MWCNT-RGO was conducted using a conventional three-electrode system. A MWCNT-GO/ITO was used as working electrode, one platinum wire was used as the auxiliary electrode and an Ag/AgCl (3M KCl) as the reference electrode. The electrochemical reduction process was applied to obtain MWCNT-RGO/ITO by immersing MWCNT-GO/ITO into 0.1 M pH 7 phosphate buffered solution (PBS) solution with cyclic sweeping in the potential range from 0.0 to -1.4 V at a scan rate of 10 mV/s for 10 cycles.

The morphology of the MWCNT-RGO thin film was characterized using a scanning electron microscope (SEM), S-4700, Hitachi High Technologies Corporation. The thickness of the thin film was measured using optical 3D profiler (ContourGT-I, Bruker). Fourier transform infrared spectroscopy (FTIR) spectra were obtained using a Nicolet 8700 FTIR spectrometer (Thermo Scientific Instrument). The optical analysis was obtained by UV-Vis spectrophotometer (Perkin Elmer Lambda 950).

RESULTS AND DISCUSSION

The morphology of MWCNT-RGO thin film was examined by SEM. Fig. 1a shows the top-view SEM image of the MWCNT-RGO thin film. It can be seen that the RGO sheets and MWCNT constructed a very dense structure. The thickness of the hybrid thin film was measured using optical 3D profiler. As shown in Fig. 1b, the 3D image clearly indicates the thickness of the hybrid thin film is approximately 1.75 μm . Moreover, the both SEM and optical 3D profiler characterization show that the constructed hybrid thin film displays a uniform surface morphology.

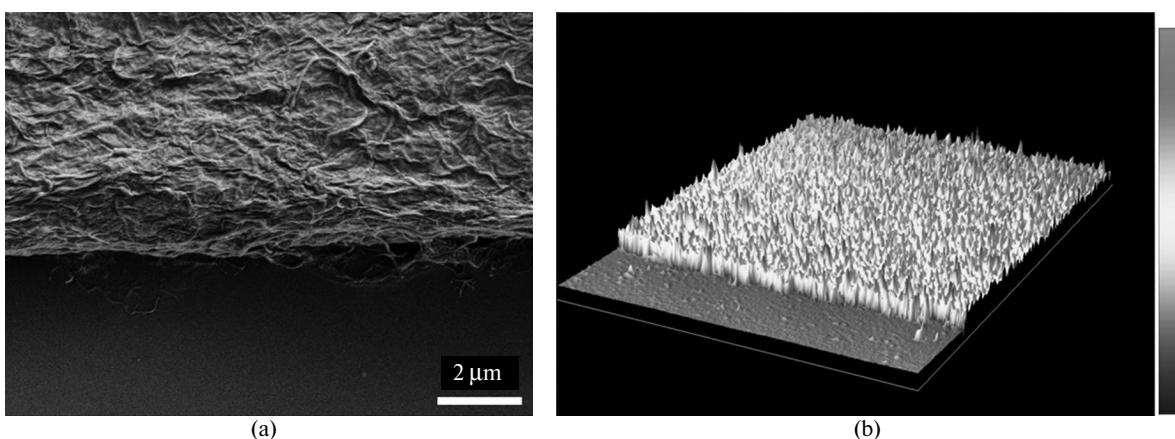


Fig. 1. SEM image (a) and optical 3D profiler image (b) of MWCNT-RGO hybrid thin film.

UV-Vis spectroscopy was used for confirming the reduction process of GO during the cyclic voltammetry (CV) scans. Figure 2a shows the UV-Vis spectra of GO and MWCNT-RGO. As expected, the spectrum of GO displays two characteristic absorption peaks at 225 and 317 nm, corresponding to $\pi-\pi^*$ transitions of aromatic C–C bonds and $n-\pi^*$ transitions of C=O bonds, respectively [35]. However, the peak at 225 nm of GO redshifts to 266 nm and the shoulder absorption peak at 317 nm disappears in the spectrum of MWCNT-RGO, indicating the GO has been reduced during the CV scans.

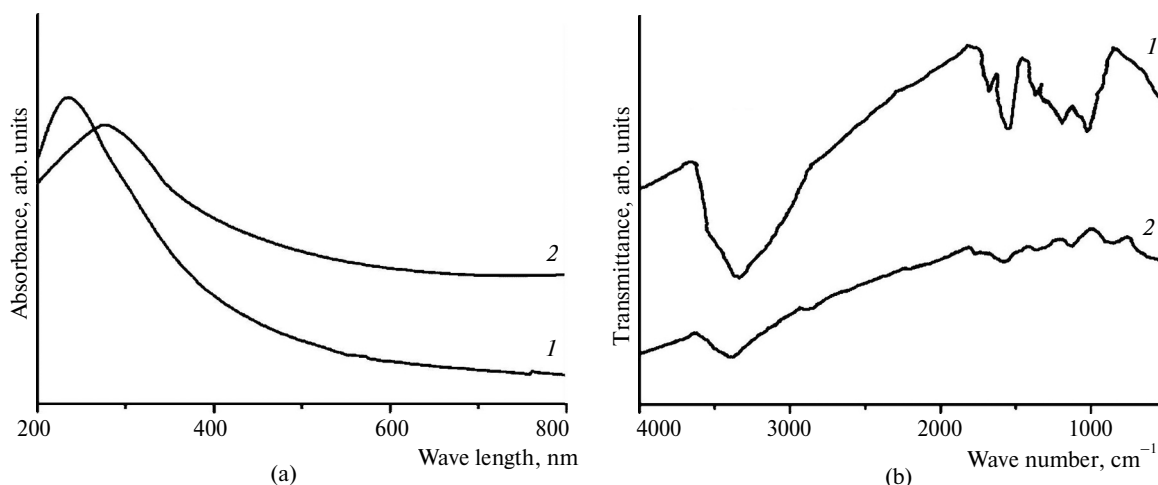


Fig. 2. UV-Vis spectra (a) of GO (1) and MWCNT-RGO (2). FTIR spectra (b) of MWCNT-GO (1) and MWCNT-RGO (2).

The reduction process was also confirmed by FTIR study. Figure 2b shows the FTIR spectra of MWCNT-GO and MWCNT-RGO. It can be seen that the spectrum of MWCNT-GO shows several characteristic peaks at 3430, 1636, 1171 and 1042 cm^{-1} corresponding to the $-\text{OH}$ vibration stretching, carboxyl $\text{C}=\text{O}$, epoxy $\text{C}-\text{O}$ and alkoxy $\text{C}-\text{O}$, respectively [36]. After CV scans, these peaks show a relatively lower intensity or even vanished in the spectrum of MWCNT-RGO, further confirming the formation of RGO.

The fabricated MWCNT-RGO/ITO was used for measuring the Hg^{2+} content in the water. Figure 3, curve 1 shows the differential pulse voltammetry (DPV) measurements recorded from 0 to 0.8 V with bare ITO, MWCNT-GO/ITO and MWCNT-RGO/ITO for analysis of 100 nM Hg^{2+} . It can be seen that the Hg^{2+} oxidation at bare ITO only exhibits a very small stripping peak. In case of MWCNT-GO/ITO, a larger peak appears at approximately 0.48 V corresponding to the Hg^{2+} oxidation. This enhancement is due to the higher surface area and better conductivity produced by MWCNT-GO hybrid thin film modified ITO, which facilitates the electrons transfer at the electrode surface. In contrast, an even higher current response is observed at MWCNT-RGO/ITO, indicating that the electrochemically reduced GO could restore its conductivity, which further enhance the electrocatalytic performance of the electrode.

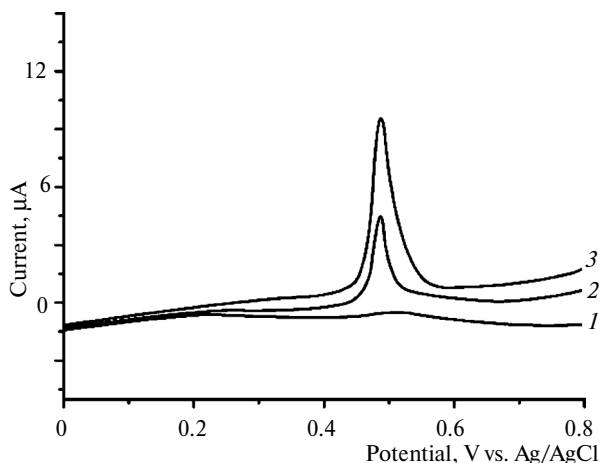


Fig. 3. DPV voltammograms of 100 nM Hg^{2+} recorded at bare ITO (1), MWCNT-GO/ITO (2) and MWCNT-RGO/ITO (3) in 0.1 M HCl.

Accumulation step is a common method for enhancing the electrochemical performance. Figure 4 shows the effect of accumulation potential and time in the Hg^{2+} detection. As shown in Fig. 4a, the highest oxidation current response is obtained at -0.20 V. The peak current increases gradually with the increase of accumulation time from 50 to 300 s and remains a similar performance if a longer accumulation time is applied (see Fig. 4b). Thus, the accumulation conditions of -0.20 V and 300 s were adopted in further measurements.

Figure 5 shows the DPV curves for various concentrations of Hg^{2+} electrochemically reacted at MWCNT-RGO/ITO recorded under optimum experimental conditions. It can be observed that the oxidation peak current of Hg^{2+} is proportional to its concentration in the range from 0.5 to 150 nM. The linear regression equation can be expressed as is $I_{pa} (\mu\text{A}) = 0.0984 c (\text{nM}) + 0.9194$, with a correlation coefficient of 0.988. The limit of detection (LOD) is estimated to be 0.05 nM at a signal-to-noise ratio of 3.

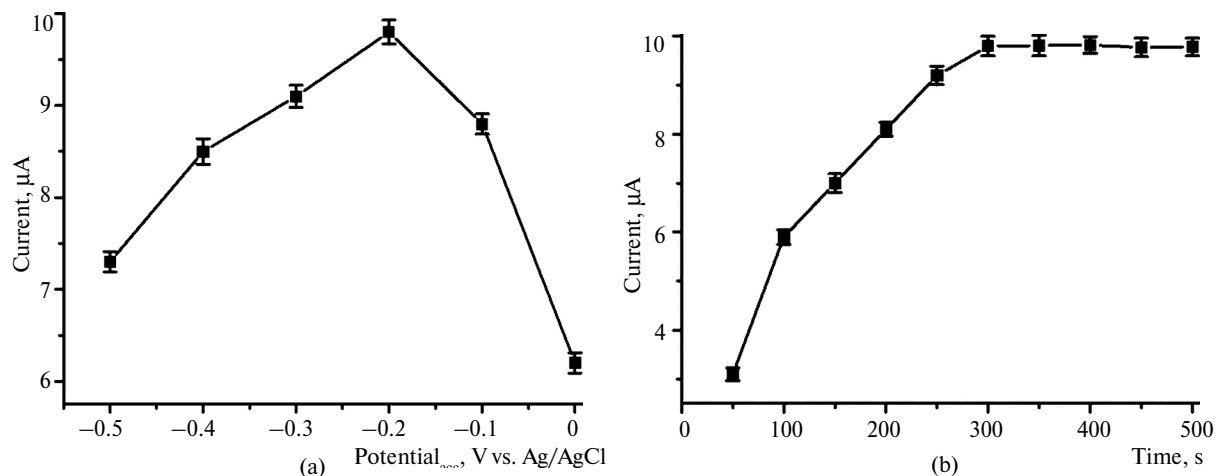


Fig. 4. Effect of the (a) accumulation potential and (b) accumulation time on the current response of 100 nM Hg^{2+} at MWCNT-RGO/ITO.

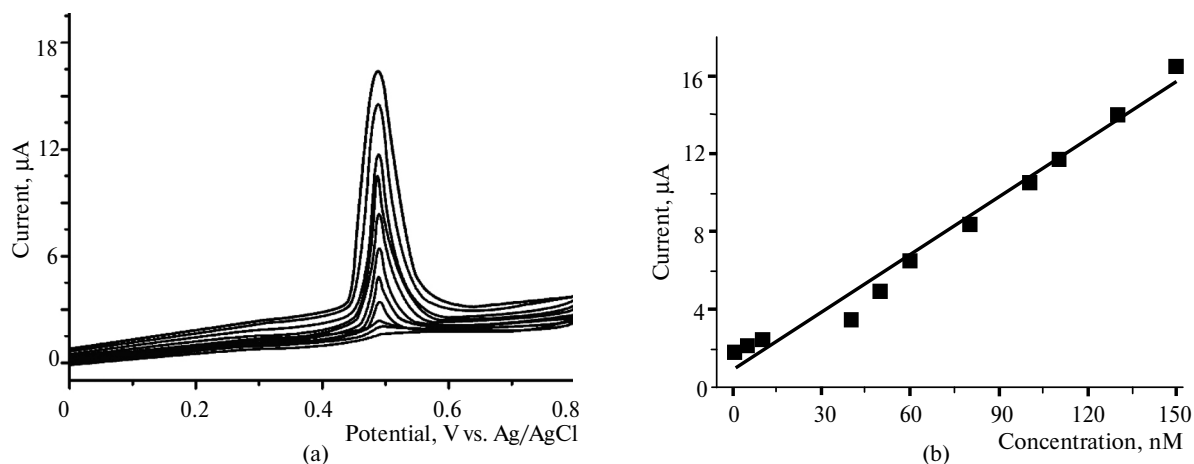


Fig. 5. DPV curves (a) of the MWCNT-RGO/ITO after the addition of various concentrations of Hg^{2+} (0, 0.5, 1, 2, 5, 10, 40, 50, 60, 80, 100, 110, 130 and 150 nM) in 0.1 M HCl. Plot of the value of anodic peak currents as a function of the concentration of Hg^{2+} (b).

As the guideline value of the Hg^{2+} in drinking water is 5 nM (World Health Organization), the proposed method is capable for real samples analysis. Therefore, we further studied the feasibility of the MWCNT-RGO/ITO for environmental and drinking water analysis. Tap water, rain water, bottle water and lake water were collected for analysis. The standard addition method was applied and the results are listed in the table. The results indicate that the recovery for the determination of Hg^{2+} is in the range of 98.1–101.9%, revealing that the proposed Hg^{2+} sensor could be employed for accurate and feasible determining Hg^{2+} in environmental water samples.

We also tested the influence of common interference species. The DPV results indicated that the 50-folds of Cd^{2+} , Cr^{3+} , Na^+ , K^+ , Zn^{2+} , Pd^{2+} , Co^{2+} , Cl^- and I^- did not interfere with the analysis of Hg^{2+} (peak current changes are less than $\pm 4\%$). Therefore, detection of Hg^{2+} in our proposed sensor is not affected by the common interferences and the selectivity of the sensor is satisfactory.

In order to study the reproducibility of the electrode preparation procedure, six freshly prepared MWCNT-RGO/ITO were tested for determination of 100 nM Hg^{2+} . The RSD for the peak currents was determined to be 3.11 %, suggesting a satisfactory reproducibility of the sensor preparation procedure. The stability of the

MWCNT-RGO/ITO was tested by storing the MWCNT-RGO/ITO in 4°C refrigerator for 1 month and then the DPV was recorded. The results showed that the oxidation current remained 96.3% for 100 nM Hg²⁺ detection compared with the original test.

Determination of Hg²⁺ in water samples using MWCNT-RGO/ITO

Water sample	Added	Found	Recovery	RSD
	nM		%	
Tap 1	0	0	—	0.25
Tap 2	5	5.02	100.4	1.11
Rain 1	0	0.20	—	1.02
Rain 2	5	5.30	101.9	2.55
Bottle 1	0	0	—	0
Bottle 2	10	10.06	100.6	2.11
Lake 1	0	0.75	—	2.33
Lake 2	10	10.55	98.1	0.23

CONCLUSIONS

In this work, a novel MWCNT-RGO hybrid thin film was prepared via a simple electro-reduction process using GO dispersed MWCNT as precursor. The prepared thin film has 1.75 μm in thickness with a uniform surface morphology. UV-Vis spectroscopy and FTIR characterizations confirmed the successful reduction during the CV scans. The prepared MWCNT-RGO/ITO was then employed for determination of Hg²⁺ in various environmental water samples. The proposed Hg²⁺ sensor exhibited a linear response range from 0.05 to 150 nM and a low detection limit of 0.05 nM.

REFERENCES

- Harada, M., *Critical Rev. Toxicol.*, 1995, vol. 25, pp. 1–24.
- Kim, H.N., Lee, M.H., Kim, H.J., et al., *Chem. Soc. Rev.*, 2008, vol. 37, pp. 1465–72.
- Galimova, V.M., Surovtsev, I.V., Mank, V.V., et al., *J. Water Chem. Technol.*, 2013, vol. 35, pp. 210–214.
- Liu, M., Wang, Z., Zong, S., et al., *ACS Appl. Mater. and Interfaces*, 2014, vol. 6, pp. 7371–79.
- Wang, Z.-X. and Ding, S.-N., *Anal. Chem.*, 2014, vol. 86, pp. 7436–45.
- Mohammadpour, Z., Safavi, A., and Shamsipur, M., *Chem. Eng. J.*, 2014, vol. 255, pp. 1–7.
- Ma, Z.-Y., Pan, J.-B., Lu, C.-Y., et al., *Chem. Commun.*, 2014, vol. 50, pp. 12088–90.
- Wei, Y., Yang, R., Liu, J.-H., and Huang, X.-J., *Electrochim. Acta*, 2013, vol. 105, pp. 218–223.
- Zhou, N., Li, J., Chen, H., et al., *Analyst*, 2013, vol. 138, pp. 1091–97.
- Palanisamy, S., Madhu, R., Chen, S.-M., and Ramaraj S.K., *Anal. Methods*, 2014, vol. 6, pp. 8368–73.
- Wu, Z., Jiang, L., Zhu, Y., et al., *J. Solid State Electrochem.*, 2012, vol. 16, pp. 3171–77.
- Lu, X., Dong, X., Zhang, K., and Zhang, Y., *Anal. Methods*, 2012, vol. 4, pp. 3326–31.
- Li, D., Li, J., Jia, X., and Wang, E., *Electrochem. Commun.*, 2014, vol. 42, pp. 30–33.
- Dago, A., Ariño, C., Díaz-Cruz, J.M., and Esteban, M., *Int. J. Environ. Anal. Chem.*, 2014, vol. 94, pp. 668–678.
- Wang, M., Yuan, W., Yu, X., and Shi, G., *Anal. Bioanal. Chem.*, 2014, vol. 406, pp. 6953–56.
- Sai-Anand, G., Gopalan, A.-I., Kang, S.-W., et al., *Sci. Adv. Mater.*, 2014, vol. 6, pp. 1356–64.
- Luo, T., He, M., Gao, C., et al., *Electrochem. Commun.*, 2014, vol. 42, pp. 26–29.
- El, Aroui F., Lahrich, S., Farahi, A., et al., *J. Taiwan Institute of Chem. Eng.*, 2014, vol. 45, pp. 2725–32.
- Stavitskaya, S.S., Vikarchuk, V.M., Kovtun, M.F., Poddubnaya, O.I., and Puziy, A.M., *J. Water Chem. Technol.*, 2014, vol. 36, pp. 110–114.
- Wang, A., Ng, H.P., Xu, Y., et al., *J. Nanomater.*, 2014, vol. 2014, pp. 6.
- Wang, A., Fu, L., Ng, H.P., et al., *J. Non-Oxide Glasses*, 2015, vol. 7, pp. 1–12.
- Novoselov, K.S., Geim, A.K., Morozov, S.V., et al., *Science*, 2004, vol. 306, pp. 666–669.
- Stankovich, S., Dikin, D.A., Dommett, G.H.B., et al., *Nature*, 2006, vol. 442, pp. 282–286.
- He, L., Fu, L., and Tang, Y., *Catal. Sci. and Technol.*, 2015, vol. 5, pp. 1115–25.
- Fu, L., Zheng, Y., Wang, A., et al., *Sensor Lett.*, 2015, vol. 13, pp. 81–84.

26. Fu, L., Zheng, Y., Wang, A., et al., *Food Chem.*, 2015, vol. 181, pp. 127–132.
27. Fu, L., Zheng, Y., and Wang, A., *Int. J. Electrochem. Sci.*, 2015, vol. 10, pp. 3518–29.
28. Zheng, Y., Fu, L., Wang, A., and Cai, W., *Ibid.*, 2015, vol. 10, pp. 3530–38.
29. Fu, L. and Fu, Z., *Ceram Int.*, 2015, vol. 41, pp. 2492–96.
30. Fu, L., Zheng, Y.-H., and Fu, Z.-X., *Chem. Papers.*, 2015, vol. 69, no. 5, pp. 655–661.
31. Hummers, W.S. and Offeman, R.E., *J. Amer. Chem. Soc.*, 1958, vol. 80, pp. 1339.
32. Gan, T. and Hu, S., *Microchim Acta.*, 2011, vol. 175, pp. 1–19.
33. Fu, L., Zheng, Y., Ren, Q., et al., *J. Ovonic Res.*, 2015, vol. 11, pp. 21–26.
34. Zheng, Y., Wang, A., Lin, H., et al., *RSC Adv.*, 2015, vol. 5, pp. 15425–30.
35. Paredes, J.I., Villar-Rodil, S., Martinez-Alonso, A., and Tascon, J.M.D., *Langmuir*, 2008, vol. 24, pp. 10560–64.
36. Liu, Z., Robinson, J.T., Sun, X., and Dai, H., *J. Amer. Chem. Soc.*, 2008, vol. 130, pp. 10876–77.